What determines the size of liquid capillary condensates below the bulk melting point?

What Determines the Size of Liquid Capillary Condensates Below the Bulk Melting Point?

P. Barber,[†] T. Asakawa,[‡] and H. K. Christenson*[,†]

School of Physics and Astronomy, University of Leeds, Leeds, LS2 9JT, U.K. and Division of Materials Sciences, Graduate School of Natural Science and Technology, Kanazawa University, Kanazawa 920-1192, Japan

Received: October 5, 2006; In Final Form: November 1, 2006

Capillary condensation from vapor has been studied at temperatures below the bulk melting point T_m of the condensing substance using a surface force apparatus. Both mica and mica modified by self-assembly of a fluorinated surfactant (perfluoro-1H,1H,2H,2H-decylpyridinium chloride) have been used as substrate surfaces. The condensing liquids, cyclooctane and menthol, nearly wet (contact angle $<15°$) mica but show a high ($\sim 60°$) contact angle on the fluorinated surface. As in previous studies with unmodified mica, we find that both cyclooctane and menthol condense as liquids below T_m, and that the size of the condensates at solid−vapor coexistence is limited and inversely proportional to the temperature depression below T_m, or ΔT. A comparison of the size of the condensates between the fluorocarbon surfaces and the mica surfaces and the quantitative dependence of the size of the condensate on ΔT for cyclooctane lead us to conclude that the maximum condensate size is determined by the equilibrium between condensed, "supercooled" liquid and vapor, and is hence proportional to the surface tension of the liquid−vapor interface. From a consideration of the equilibrium between a liquid and a hypothetical solid condensate, it is concluded that a solid condensate does not usually form for kinetic reasons although two exceptions were found in earlier work.

Introduction

Highly subdivided matter, such as substances confined to porous media, or finely dispersed particles shows phase transitions that are shifted from their bulk values.[1,2] The large surface-area-to-volume ratio causes the relative magnitudes of the surface free-energy terms to compete with bulk free-energy terms and the phase with the smaller surface or interfacial free energy will be favored. This general statement covers well-known phenomena such as capillary condensation and melting-point depression of small particles and substances in pores. Porous materials and dispersions are ubiquitous in nature and in technological applications, and both capillary condensation and melting-point (or freezing-point) depression have important practical consequences. Frost heave, weathering of rocks and man-made building materials, industrial processing of powders, metals and ceramics, and recovery of oil from reservoir rocks are some of the relevant practical areas.

Capillary condensation of liquid from undersaturated vapor occurs because the free energy of a solid−vapor interface is larger than that of a solid−liquid interface if the liquid has a contact angle of less than 90° on the solid substrate. Kinetic factors may lead to the existence of a metastable vapor phase[3,4] (e.g., in narrow slits), but in a wedge-shaped pore capillary condensation will readily take place as there is no energy barrier toward nucleation of the liquid phase. Capillary condensation in porous media is an important area of research and has been widely used to characterize porous materials[5,6] but fundamental investigations are more conveniently carried out with single pores. The surface force apparatus[7,8] (SFA) and similar devices[9] with a surface configuration of crossed cylinders or a sphere and a flat allow the study of capillary condensation in a single pore. Effects due to pore-size polydispersity, interconnectivity, and the metastable states that may result in porous networks are thus avoided.[10] Furthermore, the pore size may be varied continuously and reversibly in a single experiment. The first accurate verification of the Kelvin equation for liquids in pores was carried out with the SFA over 25 years ago,[11] and since then a considerable amount of knowledge about capillary condensation has accumulated. Although the SFA has the advantage of multiple-beam interferometry,[12] which allows the unambiguous detection of capillary condensates via refractive index differences between the condensate and the surrounding phase, a number of experiments[13,14] have been carried out with a force-measuring device that only allows the presence of a condensate to be indirectly inferred. This instrument has the advantage of greater rigidity,[9] which increases the range over which forces can be accurately measured. Both static and dynamic aspects of capillary condensation from vapor have been studied. Dynamic experiments have included studies of the mechanism of the condensation process itself,[14,15] the evaporation of liquid bridges,[16,17] the growth rates of capillary condensates,[18−20] and the effects of wetting hysteresis at the three-phase line.[21] Equilibrium experiments have extended the scope of capillary condensation studies to cover phenomena such as condensation of solute from solution,[22] condensation from vapor at temperatures below the bulk melting point T_m,[23,24] and freezing of liquid capillary condensates.[25] The atomic force microscope also has been used for capillary condensation experiments, mostly to study the effects of condensates on friction and adhesion.[26−30]

Historically, melting- and freezing-point depression in porous media was first studied by investigating capillary condensation at temperatures below the bulk melting point of the condensing substance.[1,31−34] The porous systems were usually rather ill-

* Corresponding author. E-mail: h.k.christenson@leeds.ac.uk.
[†] University of Leeds.
[‡] Kanazawa University.

10.1021/jp066556b CCC: $37.00
Published on Web 01/12/2007

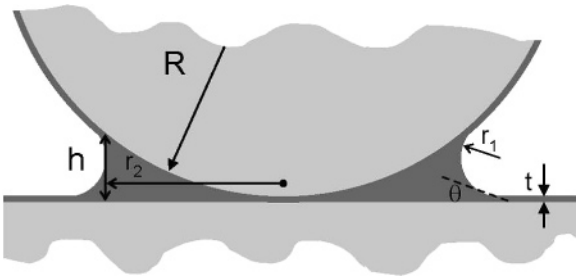

Figure 1. Schematic cross-section of the surfaces in the equivalent sphere-on-a-flat configuration in the presence of a capillary-condensed annulus. The radius of curvature of the surfaces $R \approx 2$ cm. t is the thickness of the adsorbed layer on the surfaces far from the condensate, θ is the contact angle of the liquid in the condensate on the surface, and r_1, r_2 are the principal radii of curvature of the condensate-vapor interface. Typically, $r_2 \approx 25-50$ μm and $r_1 \approx -(10-500)$ nm, so that $1/r = 1/r_1 + 1/r_2 \approx 1/r_1$. The condensate size h is related to r and t by $h = 2r \cos\theta + 3t$.

defined with a considerable polydispersity of the pore size. The freezing and melting points of capillary condensates could be identified by breaks in the vapor pressure versus temperature curves. Later, with the advent of more well-defined media (e.g., Vycor glass and related materials) most studies were carried out by allowing the porous matrix to absorb liquid above T_m and then lower the temperature.[1,2] Because of the transparency and amorphous nature of these porous media, a variety of techniques may be used (e.g., NMR, diffraction, calorimetry, light scattering, etc.). In these studies, the melting- and freezing-point depression has usually been found to be inversely proportional to the pore diameter with freezing occurring at a lower temperature than melting. A number of kinetic and thermodynamic models[35] have been advanced to explain the details of the pore-size dependence, mostly based on the Gibbs−Thomson equation. Given that a liquid phase in general wets a solid substrate in the presence of its own solid, it is favorable to keep the pore substance liquid below T_m.

In general, there is no true equilibrium with the vapor phase during these porous-media studies. Filled pores prevent free exchange of matter between vapor and condensed phases. Some exceptions have been noted, particularly with hydrogen and helium, which are in some cases able to diffuse effectively through the solid matrix.[36−38] By contrast, capillary condensation in the SFA is studied under conditions of true equilibrium with the vapor phase. In experiments carried out below T_m, it has been shown that liquid condensates form between mica surfaces for moderate temperature depressions $\Delta T = T_m - T$,[23,24] but that these are limited in size at coexistence, when the vapor is in equilibrium with bulk solid. Just as in the porous media studies, the "pore diameter", defined as the surface separation, h, at the condensate-vapor interface (see Figure 1), is inversely proportional to ΔT. Unlike in porous media studies, however, if the temperature is reduced without separating the surfaces the condensates evaporate rather than freeze[1,20] for all liquids so far studied.

In experiments with long-chain *n*-alkanes (mainly *n*-octadecane),[25] it was found that liquid condensates that formed as annuli around the contact region of the mica surfaces would freeze when these were separated. A semiquantitative correlation could be made between the relative sizes of the vapor−condensate interface and the mica−condensate interface and the ΔT at which freezing would occur on separation. An increase in the condensate−vapor interfacial area, such as occurs on separation of the surfaces, would promote freezing. A frozen condensate would remelt if the surfaces were forced into contact around the solid, thereby decreasing the condensate−vapor interfacial area and increasing the area of contact between condensate and mica. The relative ease with which freezing of bridges of *n*-octadecane occurs may be related to the phenomenon of surface freezing that is known to occur at the liquid−vapor interface of long-chain *n*-alkanes of carbon number 15 or higher.[39,40] This ordered layer promotes nucleation of solid alkane from bulk liquid and would be expected to do the same in the liquid bridges in the SFA. Freezing of liquid bridges on separation was not found with *tert*-butanol, menthol, or cyclohexanol with which surface freezing does not take place.

With *neo*-pentanol[41] and tetrabromomethane,[42] condensation of solid directly from vapor was observed, although this appeared to occur outside and around an initially condensed liquid condensate in the case of *neo*-pentanol. With *neo*-pentanol, the solid condensates grew very large close to solid−vapor coexistence, as expected because the chemical potential of the vapor is close to that of bulk solid. These results were the first direct observations of capillary condensation of solid from vapor and show that both solid *neo*-pentanol and solid tetrabromomethane must have contact angles of less than 90° on mica.

H.K.C. has previously attributed the quantitative relationship between the condensate size h (Figure 1) and ΔT for the liquid capillary condensates at coexistence to the thermodynamic instability of a solid condensate in a small mica wedge. The liquid condensate would grow until its maximum size was governed by the equilibrium between a liquid condensate and a hypothetical solid condensate. On the assumption that the liquid in the condensate would wet the mica substrate in the presence of its solid, the relationship between the condensate size h at coexistence and ΔT would be[23]

$$\frac{1}{h} = \frac{\Delta H_{fus} \Delta T}{4 V_{ML} \gamma_{SL} T_m} \tag{1}$$

where ΔH_{fus} is the enthalpy of fusion, V_{ML} is the molar volume of the liquid, and γ_{SL} is the interfacial tension between liquid and solid of the condensing substance. This equation is identical to the Gibbs−Thomson equation for a cylindrical pore of diameter h. In this model, it was assumed that further growth could only occur by direct condensation of solid outside the liquid annulus, as was found with *neo*-pentanol.[41]

The previous studies of capillary condensation below T_m have all been carried out with mica surfaces and the condensing liquids have had small (<10°) contact angles on the mica. To investigate the effect of the nature of the surface on capillary condensation below T_m, we set out to study a system in which the condensing liquid has a significant contact angle on the surface. We modified the mica surface by adsorbing a fluorocarbon surfactant to it and by choosing a hydrocarbon as the condensing liquid we were able to maximize the contact angle on the surface without compromising the stability of the monolayer. Cyclooctane was used as the condensing liquid because its melting point, which is close to room temperature, and its reasonably high vapor pressure are experimentally convenient. We carried out experiments both with bare mica surfaces and with mica surfaces modified by adsorption from solution of the fluorocarbon surfactant.

In the course of these experiments it became apparent that relating the condensate size to a solid−liquid equilibrium only could not be correct, and that the liquid−vapor equilibrium must also be considered. We therefore carried out some additional experiments with previously studied substances using menthol

TABLE 1:[a]

condensing substance	melting point (°C)	boiling point (°C)	ΔH_{fus} (kJ mol^{-1})	p_s (Torr at T_m)	V_M (cm^3)	γ_{LV} (mN/m)
cyclooctane	14.3	149	2.41	3	134	31
tert-butanol	25.5	82	6.70	40	94	20.7
menthol	34	212	12.4	0.1 (est)	176	(34)[b]

[a] Data are from ref 44 except the heat of fusion and vapor pressure of cyclooctane, which are from ref 52, and the heat of fusion of menthol, which is from ref 25. The surface tension of cyclooctane was measured in this study. [b] Value for cyclohexanol is from ref 53.

as the condensing liquid both with bare mica surfaces and with fluorocarbon-coated surfaces, and *tert*-butanol with mica only. The results have led us to conclude that the maximum size of the liquid condensates is governed by the equilibrium between vapor and what may be regarded as supercooled liquid with an additional reduction in chemical potential due to the curved liquid−vapor interface.

Materials and Methods

Synthesis of Fluorinated Surfactant. The fluorinated surfactant was prepared as described previously[43] by refluxing anhydrous pyridine with perfluoro-1H,1H,2H,2H-decyl iodide (Aldrich). The precipitated perfluoro-1H,1H,2H,2H-decylpyridinium iodide was washed with diethyl ether and recrystallised from acetone. The corresponding chloride was obtained by ion exchange using Amberlite IRA-410 and recrystallised from acetone.

Liquids. The cyclooctane (99+%) was from Lancaster Chemicals while the menthol (2-isopropyl-5-methyl-1-cyclohexanol, 99%) and the *tert*-butanol (2-methyl-2-propanol, 99.5%) were purchased from Sigma Aldrich. The menthol and *tert*-butanol were used as received, but in some experiments the cyclooctane was distilled under vacuum before use. No difference in the experimental results was found between distilled and undistilled cyclooctane. Some relevant physical properties of the liquids are given in Table 1.

Surface Preparation. The mica (Paramount, New York) was cleaved, cut with a hot platinum wire and was coated with 52 nm of silver by vacuum evaporation. The mica surfaces were glued to cylindrically polished silica discs of 2 cm radius of curvature with a thermosetting epoxy resin (Epikote 1004). For experiments with fluorocarbon-coated surfaces, perfluoro-1H,1H,2H,2H-decylpyridinium chloride then was adsorbed to the mica by immersing the silica discs with attached mica surfaces in a 1.0×10^{-4} M (approximately 1/10 of the cmc) aqueous solution in Millipore water for 24 h. The discs were then withdrawn, rinsed with water and cyclohexane, and blown dry with a nitrogen stream. Surfactant-coated surfaces for characterization studies were prepared from thicker, freshly cleaved mica pieces in an identical fashion.

Surface Characterization. The fluorocarbon surfaces were characterized by contact angle measurements before and after exposure to various liquids and by atomic force microscopy (AFM) scans. The AFM scans showed a flat, completely featureless surface. If part of the mica surface was masked by a second piece of mica during adsorption, the step height at the edge of the surfactant layer after the masking mica piece was removed was found to be 1.2−1.3 nm. The length of the molecule was estimated from atomic dimensions to be 1.4 nm, suggesting a reasonably well-packed monolayer surface.

The contact angle measurements were carried out with a FTÅ2000 instrument from First Ten Ångstroms. The advancing contact angle of water on the fluorocarbon surface θ_a was 93 ± 2° and the receding angle θ_r was 18 ± 2°. θ_a for cyclooctane was 62 ± 1° and θ_r was 50 ± 2° on the fluorocarbon surface. The contact angle of a cyclooctane droplet placed on the surface was unchanged (to within ±2°) for periods of up to 5 h, suggesting little effect of cyclooctane on the integrity of the monolayer. For menthol, the contact angles were $\theta_a = 57 \pm 2°$ and $\theta_r = 45 \pm 2°$. With *tert*-butanol, however, the contact angle on the fluorocarbon surface decreased significantly on exposure to the liquid and these surfaces were not used for condensation experiments with *tert*-butanol. The contact angles of cyclooctane on mica were $\theta_a = 15 \pm 2°$ and $\theta_r = 8 \pm 2°$.

The FTÅ2000 also was used to measure the surface tension of cyclooctane and a value of 31 mNm^{-1} at 22 °C was obtained.

SFA Experiments. A surface force apparatus based on the Mark IV version[8] was used to study capillary condensation between mica surfaces and between fluorocarbon-coated mica surfaces. The surfaces are mounted as crossed cylinders and their separation controlled with a micrometer/translation stage and a piezoelectric cylinder. One of the surfaces is rigidly mounted on the piezoelectric cylinder and the second surface is mounted at the end of a very rigid cantilever of approximate spring constant 10^5 Nm^{-1}. The surface separation and refractive index of the medium between the surfaces is determined by multiple-beam interferometry.[12] Discrete wavelengths transmitted by the opposing, back-silvered mica surfaces are resolved in a grating monochromator, recorded with a charge-coupled device (CCD) camera at the exit slit, and are analyzed with the standard three-layer interferometry equations.

The temperature was controlled using a system based on a design by Heuberger et al.[44] The apparatus was housed in a Styrofoam-insulated wooden box whose temperature could be controlled and varied by means of Peltier elements. The lowest achievable temperature with the system was 7 °C for short periods of less than 1 h and 8 °C for longer periods.

The typical experimental procedure was to determine first contact between the surfaces in dry nitrogen with molecular sieve 3A as the drying agent in the chamber. In the case of cyclooctane, liquid was injected onto the molecular sieve in the apparatus above T_m and the chamber was allowed to equilibrate overnight at 30 °C to increase the evaporation rate. The apparatus was then kept overnight in a refrigerator/freezer at −5 °C to ensure that the reservoir would freeze (substantial undercooling may occur with cyclooctane), which was checked by visual inspection. In some experiments, a few measurements were made with unfrozen liquid in the chamber at various temperatures to note the effect of an undercooled liquid reservoir on the condensate size.

The apparent vapor pressure, as determined with the Kelvin equation above T_m varies slightly with the total amount of cyclooctane injected. The amount injected was 0.5 or 1.0 cm^3. Although the amount required to saturate the chamber is only about 0.03 cm^3, an unknown amount is absorbed by the molecular sieve and on other surfaces. There are also small (<0.1 °C) temperature gradients in the chamber, and the net effect is that the apparent vapor pressure, although close to saturation, increases slightly with the amount of injected cyclooctane. Near coexistence the equilibration time became very long (≥3 h) and the smaller amount was therefore injected in most experiments to avoid excessive equilibration times, which may lead to irreversible deformation of the curved surfaces after prolonged contact. The experiments were usually carried out by increasing the temperature from run to run but on a few occasions the temperature was decreased.

The experiments with menthol and *tert*-butanol were carried out in a similar fashion. With the higher melting point and vapor

pressure of *tert*-butanol, measurements could commence after overnight equilibration at room temperature. As menthol is solid at room temperature, a small amount (<1 g) was introduced through an access port in the side of the chamber while in a laminar flow cabinet.

After equilibration, the surfaces were brought together in the vapor phase of the studied liquids until an inward jump occurred at a separation of the order of 15−20 nm. The formation of the capillary condensate pulled the surfaces together and the condensate then continued to grow in the annular region surrounding the contact between the flattened surfaces (see Figure 1). The condensates were left until no further growth was apparent and their equilibrium size measured by locating the discontinuity in the fringes found at the position of the condensate-vapor interface. This involves some extrapolation of the fringes as there is usually a region in which the fringe intensity is very low. The error bars in the figures are due to differences in the results of the extrapolation from the vapor phase and the extrapolation from the condensed phase. The surfaces then were separated and the condensates snapped at some large separation and then were left to evaporate. Corrections for the thermal expansion of mica were obtained by monitoring the shift in the contact position in nitrogen with temperature. The flow of the condensates during separation proves their liquid nature, and in some cases the refractive index of the cyclooctane was measured after separation. The results of four separate measurements were 1.453 ± 0.006, 1.458 ± 0.002, 1.466 ± 0.007, and 1.450 ± 0.006, close to the literature value of 1.4584 for liquid cyclooctane.[45] (The value for solid cyclooctane would be expected to be several percent higher, as found previously for solid *n*-octadecane compared to the liquid.[25]) The temperature was then changed and the procedure repeated when the apparatus and its surrounding had come to thermal equilibrium, usually after leaving the system overnight.

Results

Previous studies of capillary condensation in the SFA have mostly dealt with liquids that wet or nearly wet the substrate (mica).[11,15−20,23−25] The large (62°) contact angle of cyclooctane on the fluorocarbon surface leads to some differences in behavior compared to the condensates with small contact angles. When the fluorocarbon surfaces are separated, the annular condensate becomes a bridge that then ruptures at a large separation to form a droplet on each of the two surfaces, as usual. Because of the high contact angle, however, these droplets do not spread out over the surface as is the case with droplets on mica surfaces and the evaporation of the droplets is consequently much slower (as the radius of curvature of the droplets is many microns, the increased vapor pressure is negligible). At the location of the droplets the interference fringes show a gap (see Figure 2) which we believe is due to a combination of total internal reflection close to the perimeter of the droplets and deviation of the light beam near its center. If the droplets are allowed to coalesce by bringing the surfaces closer, the part of the interference fringes that corresponds to the bridge reappears as there is now much less effect on the light beam.

The separation at which the surfaces were pulled together was in the range 10−25 nm, depending on the temperature. The larger values were found for the higher temperatures at which the thickness of the adsorbed films on the surfaces is greater. There was no change in this separation during the course of an experiment and we take this as evidence that no significant contamination of the condensates or disruption of the fluorocarbon monolayers occurred during the experiments. Both with

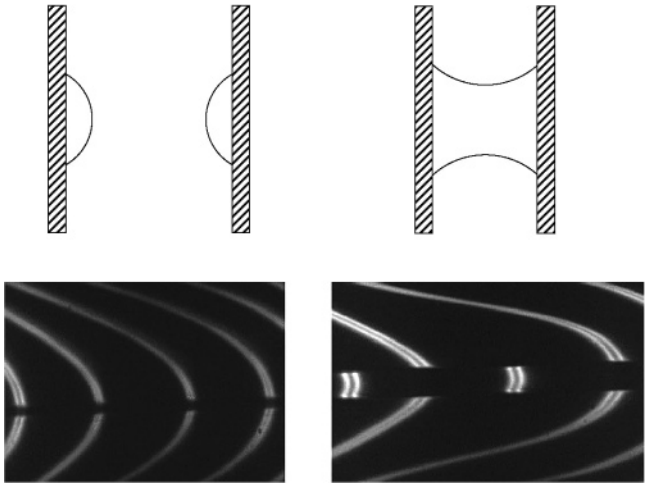

Figure 2. Appearance of the interference fringes (bottom) with mica surfaces coated with an adsorbed layer of heptadecafluorodecylpyridinium chloride and a schematic configuration of the cyclooctane condensates deduced therefrom (top). The left-hand images show the fringes and surfaces when a bridging capillary condensate of cyclooctane has snapped, leaving a droplet of high-contact angle on either surface. There is a gap at the center at which the light has been reflected or deviated by the liquid−vapor interface of the droplets. The right-hand image shows the fringes and surfaces when the two droplets have coalesced at a smaller separation. The light can now pass through the bridge, but the center part is shifted in wavelength due to the difference in refractive index compared to the surrounding vapor.

the mica surfaces and the fluorocarbon surfaces, the contact between the surfaces in the condensates was shifted outward with respect to contact in dry nitrogen, typically by about 2 nm for the mica surfaces and less than 1 nm for the fluorocarbon surfaces. This is undoubtedly because of the repulsive barriers of a solvation force both in the case of mica and the fluorocarbon surfaces, as was verified by pushing the surfaces together under high loads and observing inward jumps of 0.7 ± 0.1 nm, approximately the mean diameter of the cyclooctane molecule. The surfaces could not be pushed closer than 0.7 ± 0.1 nm from contact with either surface. As this was not studied in detail, we cannot exclude the possibility of a slight swelling of the fluorocarbon surfaces in the cyclooctane, as has been reported for some monolayer surfaces in hydrocarbon vapors and condensates.[46] Such a swelling does seem unlikely, however, in view of the large contact angle of the cyclooctane on the fluorocarbon surface and the lack of such a swelling in a study with a different fluorocarbon monolayer surface.[46]

Figure 3 shows the inverse of the measured condensate size $1/h$ as a function of ΔT for cyclooctane condensing on mica, and for cyclooctane condensing on the fluorocarbon surface. These values of h are the distance defined in Figure 1, or the separation between the surfaces at the perimeter of the annular condensate, and thus include adsorbed layers of thickness t present on the surfaces on the vapor side of the interface and any possible swelling of the monolayers discussed above. As can be seen, $1/h$ increases approximately linearly with ΔT for both surfaces. There are two sets of data (open symbols) for the mica surfaces, corresponding to 1.0 (lower set) and 0.5 cm^3 of liquid cyclooctane in the chamber, and with the smaller amount the vapor is clearly off solid coexistence as the condensate remains of finite size near T_m. From this condensate size, the relative vapor pressure obtained from the Kelvin equation was $p/p_0 = 0.993$. With the fluorocarbon surfaces (solid symbols) only the smaller amount was used to avoid the excessively long equilibration times that were required near coexistence, and the condensate size h at T_m gives $p/p_0 = 0.994$.

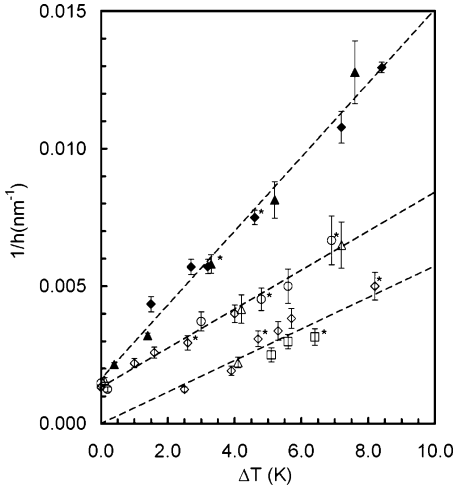

Figure 3. Measured condensate size h of cyclooctane as a function of temperature depression below the melting point ΔT. The lower set of symbols are measurements with bare mica surfaces and 1 cm^3 of cyclooctane injected into the chamber, giving $p/p_0 \approx 1$, the middle set are measurements with bare mica surfaces and 0.5 cm^3 of cyclooctane, and the upper set (filled symbols) are measurements with 0.5 cm^3 of cyclooctane with mica coated with an adsorbed layer of heptadecafluorodecylpyridinium chloride. The different symbols within each set are results from different experiments. Symbols marked with an asterisk denote measurements made on decreasing the temperature, all others were made on increasing the temperature. The lines are least-squares fits to the data sets in which the fit to the results with bare mica surfaces with 1 cm^3 of cyclooctane has been constrained to pass through the origin; the other two are free fits. The error bars are because of the difficulty of accurately locating the interference fringe discontinuities at the condensate-vapor interface at which there is generally a region of low fringe intensity.

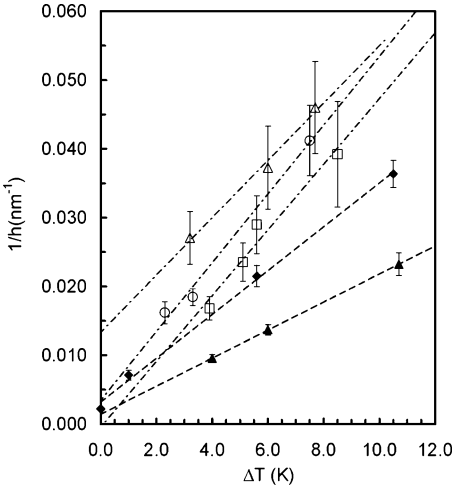

Figure 4. Measured condensate size h of menthol (filled symbols) and *tert*-butanol (open symbols) as a function of temperature depression below the melting point ΔT. The filled triangles are measurements with bare mica surfaces, and the filled diamonds are measurements mica bearing an adsorbed layer of heptadecafluorodecylpyridinium chloride. The three different open symbols are measurements at different relative vapor pressures of *tert*-butanol on bare mica. The lines are unconstrained least-squares fits to each set of data. The error bars are as in Figure 3.

The condensate sizes are thus about the same at T_m for the two different surfaces, but they deviate increasingly at lower temperatures. Each data set is from several different experiments and distinguished by different symbols. The points marked with an asterisk were taken on decreasing the temperature and all others on increasing the temperature from the lowest (greatest value of ΔT). The dashed lines are least-squares fits to the data points, although the line for the mica surfaces at coexistence has been constrained to pass through the origin (no data was collected close to T_m as the equilibration times became excessively long).

With undercooled cyclooctane in the reservoir the condensates grow very large and appear to continue growing with no clear indication of an approach to equilibrium. We did not attempt to determine accurately the condensate size in this case.

Figure 4 shows $1/h$ vs ΔT for menthol on bare mica (solid triangles) and on the fluorocarbon surface (solid diamonds). Also shown are results with *tert*-butanol and bare mica surfaces for 3 different volumes of injected liquid: 1, 3, and 5 cm^3. The broken lines are least-squares fits to the data. Clearly, the largest amount gives results that appear to extrapolate to a very large condensate size at T_m, indicating that the vapor phase is close to saturation. The other two amounts gave vapor pressures of 0.998 and 0.988, as estimated from the extrapolated condensate size and the Kelvin equation. The occurrence of inward jumps and adsorbed layers on the surfaces were noted with menthol and *tert*-butanol but we did not study this in detail.

Discussion

Previous measurements of the condensate sizes of *tert*-butanol, *neo*-pentanol, and menthol below T_m by one of us have been discussed in terms of an equilibrium between a solid condensate and a liquid condensate below T_m.[23,24] According to this model, the equilibrium condensate size would vary as

$$\frac{1}{h} = \frac{\Delta T \Delta H_{fus}}{4 T_m V_{ML} (\gamma_{SW} - \gamma_{LW})} \tag{2}$$

where ΔH_{fus} is the enthalpy of fusion of the condensing substance, V_{ML} is its molar volume, and γ_{SW}, and γ_{LW} are the free energies of interface between the wall (mica) and a solid condensate, and the interface between the wall and a liquid condensate, respectively. If ϕ is the contact angle of the liquid forming the condensate on the wall (mica) against its own solid, and this liquid is assumed to wet the wall in the presence of the solid, then

$$\gamma_{SW} - \gamma_{LW} = \gamma_{SL} \cos \phi = \gamma_{SL} \tag{3}$$

where γ_{SL} is the interfacial tension between solid and liquid of the substance in the condensate. (Note that ϕ is different to the contact angle θ, which we use for the contact angle of a liquid on the solid substrate (mica or fluorocarbon-coated mica) in vapor). Equation 2 thus reduces to eq 1 (see Introduction), and the slope of $1/h$ versus ΔT would be proportional to the interfacial tension between solid and liquid. With this analysis, γ_{SL} was found to be 14 mNm^{-1} for both *tert*-butanol and *neo*-pentanol and 25 mNm^{-1} for menthol. Unfortunately, there is no literature data on γ_{SL} for these or similar compounds with which to compare. The repeat measurements with *tert*-butanol at $p/p_0 \approx 1$ presented here in Figure 3 would give a similar value of γ_{SL} or 13 mNm^{-1}.

Application of eq 3 to the data obtained with cyclooctane (1.0 cm^3 injected volume) between bare mica surfaces (Figure 3) gives $\gamma_{SL} = 23$ mNm^{-1}. This value is five times larger than the 4.6 mNm^{-1} estimated for cyclohexane from melting-point depression studies with porous glasses.[47] Note that relaxation of the assumption that $\cos \phi = 1$ in eq 3 could only further increase this value.

Furthermore, from the slope of the $1/h$ versus ΔT fit for cyclooctane between the fluorocarbon surfaces, one calculates $\gamma_{SL} = 13$ mNm^{-1}, which is a different value for the same liquid!

This difference between the bare mica surface and the fluorocarbon surface could conceivably be accounted for by a difference in the contact angle ϕ on the two surfaces (e.g., if ϕ were 0° on the mica and about 60° on the fluorocarbon surface) but we have no evidence for this. The same holds for menthol when comparing the data obtained with the two surfaces (Figure 4). One has to postulate a much higher contact angle ϕ on the fluorocarbon surface, with no evidence for or against this.

Another problem with the previous analysis is the difficulty of quantitatively accounting for data off coexistence (i.e., when the vapor phase is not saturated). The intercept of $1/h$ must give the condensate size at the melting point, which via the Kelvin equation gives the relative vapor pressure at the melting point.[41] Equation 1, however, apparently has no dependence on the vapor pressure and it is not obvious how it would be modified to account for the condensate size off solid−vapor coexistence.

The improbably high value of γ_{SL} for cyclooctane predicted by eq 1 has led us to reconsider the factors determining the condensate size. Several experimental observations point to the fact that the equilibrium with the vapor phase is involved. These are: (1) The condensates respond to a lowering of the temperature by reducing their size via evaporation. Freezing of an annular condensate between surfaces in contact has not been observed with any studied liquid. (2) The size (h) of the condensates, both for cyclooctane and menthol, seems to scale approximately with the contact angle of the liquid on the surface against the vapor phase, which is a measurable quantity. (3) The slopes of the $1/h$ vs ΔT curves in Figures 2 and 3 seem to be similar irrespective of the exact vapor pressure and extrapolate to give a vapor pressure apparently consistent with the Kelvin equation at $\Delta T = 0$. (4) With undercooled cyclooctane in the reservoir, the condensates appear to grow without bounds, as expected if the equilibrium curvature of the condensate is zero as for the liquid in the reservoir.

The equilibrium between vapor and both liquid and solid capillary condensates below T_m was considered by Batchelor and Foster[34] in 1944. They assumed that the vapor pressure over the condensates could be obtained by a combination of the Clausius−Clapeyron equation and the Kelvin equation. The former allows extrapolation of the vapor pressure to temperatures below T_m, and together with the latter this allows the equilibrium vapor pressure of a curved liquid (or solid) interface below T_m to be determined. We have adapted their approach but consider only liquid condensates in what follows (a similar treatment is to be found in ref 42).

The saturation vapor pressure over (supercooled) liquid p_L and the saturation vapor pressure over solid p_S at a temperature T below T_m are

$$\ln\left(\frac{p_m}{p_L}\right) = -\frac{\Delta H_{vap}}{R}\left(\frac{1}{T_m} - \frac{1}{T}\right) \tag{4}$$

and

$$\ln\left(\frac{p_m}{p_S}\right) = -\frac{\Delta H_{sub}}{R}\left(\frac{1}{T_m} - \frac{1}{T}\right) \tag{5}$$

respectively. Here, ΔH_{vap} and ΔH_{sub} are the enthalpies of vaporization and sublimation, respectively, and p_m is the vapor pressure at T_m. Equations 4 and 5 together give

$$\ln\left(\frac{p_L}{p_S}\right) = -\frac{(\Delta H_{sub} - \Delta H_{vap})}{R}\left(\frac{1}{T_m} - \frac{1}{T}\right) = -\frac{\Delta H_{fus}}{R}\left(\frac{1}{T_m} - \frac{1}{T}\right) \tag{6}$$

where ΔH_{fus} is the latent heat of fusion. A vapor pressure p off coexistence at a temperature T can be related to p_L at that temperature via the Kelvin equation

$$\ln\left(\frac{p_L}{p}\right) = -\frac{V_{ML}\gamma_{LV}}{r_L RT} \tag{7}$$

where the V_{ML} is the molar volume of the condensing liquid and r_L is the curvature of the liquid−vapor interface (negative for a wetting liquid). For a liquid capillary condensate in equilibrium with vapor at a pressure p we can write

$$\ln\left(\frac{p_L}{p_S}\right) = \ln\left(\frac{p_L}{p}\right) - \ln\left(\frac{p_S}{p}\right) = -\frac{V_{ML}\gamma_{LV}}{r_L RT} - \ln\left(\frac{p_S}{p}\right) \tag{8}$$

which with eq 6 gives

$$-\frac{\Delta H_{fus}}{R}\left(\frac{1}{T_m} - \frac{1}{T}\right) = -\frac{\Delta H_{fus}}{R}\left(\frac{T - T_m}{TT_m}\right) = -\frac{V_{ML}\gamma_{LV}}{r_L RT} - \ln\left(\frac{p_S}{p}\right) \tag{9}$$

Introducing $\Delta T = T_m - T$, and $r = |r_L|$ (since the net curvature is negative) gives

$$\frac{\Delta H_{fus}\Delta T}{RTT_m} = \frac{V_{ML}\gamma_{LV}}{rRT} - \ln\left(\frac{p_S}{p}\right) \tag{10}$$

which rearranges to

$$\frac{1}{r} = \Delta T\left[\frac{\Delta H_{fus}}{V_{ML}\gamma_{LV}T_m} - \frac{R}{V_{ML}\gamma_{LV}}\ln\left(\frac{p_S}{p}\right)\right] + \frac{RT_m}{V_{ML}\gamma_{LV}}\ln\left(\frac{p_S}{p}\right) \tag{11}$$

This is total interfacial radius of curvature of a liquid condensate in equilibrium with vapor below T_m. The intercept is equal to $1/r_m$, or the inverse Kelvin radius at T_m, as expected. For $p = p_S$, eq 11 reduces to

$$\frac{1}{r} = \frac{\Delta H_{fus}\Delta T}{V_{ML}\gamma_{LV}T_m} \tag{12}$$

This equation gives the radius of curvature of a liquid capillary condensate in equilibrium with saturated vapor below T_m.

Our experimentally measured quantity h can be related to the net radius of curvature of the condensate by first noting that $1/r = 1/r_1 + 1/r_2 \approx 1/r_1$ (see Figure 1). In the absence of an adsorbed film on the surfaces, elementary geometry gives $h = 2r_1 \cos\theta = 2r \cos\theta$. The presence of an adsorbed film of thickness t may be taken into account using[48,49]

$$h = 2r\cos\theta + 3t \tag{13}$$

We have thus converted the measured condensate sizes h to interfacial radii of curvature r by using the measured values of the advancing contact angle on the fluorocarbon surfaces and subtracting three times the adsorbed film thickness on an isolated surface close to coexistence ($1 < t < 2$ nm, depending on the temperature). The data for 0.5 cm^3 cyclooctane, converted with eq 13, are plotted as $1/r$ versus ΔT in Figure 5, and the menthol and *tert*-butanol data are shown in Figure 6. The adsorbed film thicknesses for menthol and *tert*-butanol were taken from previous studies.[41,50]

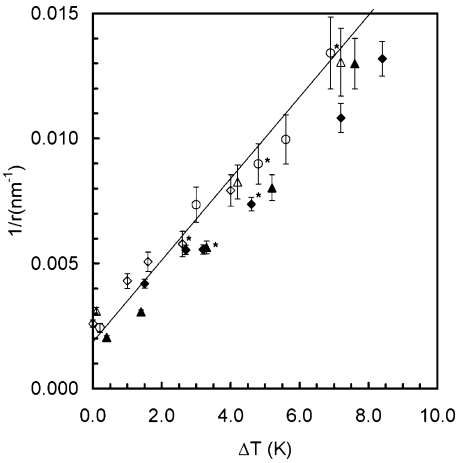

Figure 5. The radius of curvature of the condensate-vapor interface as a function of ΔT for cyclooctane condensing from undersaturated vapor on bare mica (open symbols) and on mica coated with heptadecafluorodecylpyridinium chloride (filled symbols). The data on the condensate size from Figure 3 has been corrected for the contact angle and adsorbed layer thickness using eq 13. The solid line is the prediction of eq 11, using bulk data from Table 1.

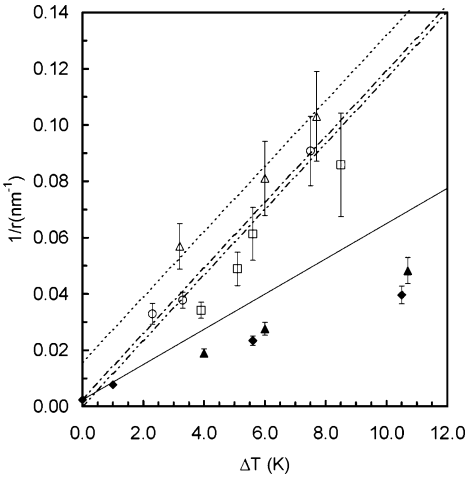

Figure 6. The radius of curvature of the condensate-vapor interface as a function of ΔT for *tert*-butanol (open symbols) condensing from undersaturated vapor on bare mica and of menthol condensing on bare mica (filled triangles) and on mica coated with heptadecafluorodecylpyridinium chloride (filled diamonds). The data on the condensate size from Figure 4 has been corrected for the contact angle and adsorbed layer thickness using eq 13. The lines are the predictions of eq 11, using bulk data from Table 1.

It is clear that normalization by the contact angle has brought each of the pair of data sets on the two different surfaces, both with cyclooctane and menthol, close together. The two data sets for menthol are indistinguishable, while for cyclooctane they are still somewhat separated from each other. Subtraction of the adsorbed film thicknesses has noticeably affected the data distribution for the smaller condensates, especially with *tert*-butanol but has little effect for cycloctane as $r, h \gg t$.

Equation 11 also has been plotted in Figures 5 and 6 with literature values of the surface tension, enthalpy of fusion, molar volume, and melting point for the respective liquids (see Table 1). As no literature value of the surface tension of menthol could be found, we have used the value for cyclohexanol (Table 1). The p/p_S has been calculated from the Kelvin equation and the value of r at or extrapolated to $\Delta T = 0$. The measured cyclooctane data in Figure 5 are reasonably close to the predictions of eq 11, although the smaller condensates appear to be slightly larger (smaller value of $1/r$) than expected. Least-squares fits to the experimental data sets would give $\gamma_{LV} = 38$ mNm^{-1} for cyclooctane and $\gamma_{LV} = 50$ mNm^{-1} for menthol, which is too large by 19% for cyclooctane and probably too large by at least the same percentage for menthol. For *tert*-butanol, fits give $\gamma_{LV} \approx 20$, which is close to the literature value, for the three series of data points, although the error is obviously quite large because of the large error bars and small number of points in each set. Results from previous studies of condensate sizes when analyzed with eq 11 or 12 (using $h = 2r$) would give $\gamma_{LV} = 26$ mNm^{-1} for *tert*-butanol,[23] $\gamma_{LV} = 28$ mNm^{-1} for *neo*-pentanol,[23,41] and $\gamma_{LV} = 48$ mNm^{-1} for menthol.[41] However, the thickness of adsorbed films on the mica surfaces was included in h ($= 2r + 3t$) in these studies and if eq 13 were employed to correct for this the results would become closer to the true values of γ_{LV}.

It is unlikely that the approximations inherent in the Clausius−Clapeyron equation, chiefly neglect of the different heat capacities of the liquid and solid phases, are responsible for the discrepancy between the experimental results and those expected from eq 11 or 12. In the case of water, it has been estimated that for $\Delta T = 10$ K this would lead to a 3% error in interfacial tension calculated from the Gibbs−Thomson equation[51] and this may confidently be taken as a maximum error because of this approximation in these experiments.

Any uncertainty in T_m itself also would influence the effective slope of a fit to the data points. We simply have used literature values and only checked that these correspond approximately to the actual T_m.

The surface tension itself decreases with temperature, but for liquids such as those studied here the effect is of the order of 1 mNm^{-1} over 10 °C and cannot account for any significant part of the discrepancy between our model and the experimental results. In many porous-media studies, the effect of a nonfreezing layer of liquid next to the walls has been considered, which leads to an enthalpy of fusion that decreases with pore size. It is unclear if this needs be considered here as the condensates never actually freeze, although the enthalpy of fusion enters into the derivation of eq 11 (see eq 6).

The error may well be because of some slight dissolution of solute in the condensates, which might be expected to have a larger effect with the smaller condensates. This would lead to an additional depression of the melting point beyond that caused by the curved interface. If this solute comes from the surface its concentration would moreover vary as $1/h$ and the additional reduction in T_m also would be inversely proportional to the interface curvature. However, the fact that the slope of the cycloctane data is approximately equal for both the mica surfaces and the fluorocarbon surfaces suggests that there is no significant dissolution of the adsorbed fluorocarbon surfactant.

Despite these uncertainties, we believe that the data for cyclooctane on both mica and the fluorocarbon surface are consistent with the condensate size being determined by the liquid−vapor equilibrium. The disagreement for menthol is slightly larger although in view of the lack of surface tension data it may be unwise to speculate further on this. For *tert*-butanol, the scatter is fairly large, but all three data sets are consistent with the use of eq 11 and different relative vapor pressures.

If we accept that the maximum size (in terms of r) of a liquid condensate in equilibrium with vapor is given by eq 12, it is interesting to compare quantitatively with the predictions of eq 1. This equation should be valid for the solid−liquid equilibrium

of a condensate at saturation and predicts that a wetting condensate should be metastable toward freezing if $\gamma_{LV} > 2\gamma_{SL}$ in which case the outer part of the condensate may freeze. Neglecting the small difference between h and $2r$ for a wetting liquid (eq 13), at equilibrium an inner liquid condensate should be surrounded by a solid condensate for

$$\frac{4T_m V_{ML}\gamma_{SL}}{\Delta H_{fus}\Delta T} < h < \frac{2T_m V_{ML}\gamma_{LV}}{\Delta H_{fus}\Delta T} \qquad (14)$$

Whether or not this is thermodynamically possible will depend on the contact angle of the solid on the substrate in vapor. If it exceeds 90° (or equivalently $\gamma_{SW} > \gamma_{VW}$), a solid condensate would be unstable toward evaporation and could not form. Even if the contact angle of the solid on the substrate were less than 90°, freezing would be controlled by kinetics and may not occur in the absence of a suitable nucleation mechanism. Conceivably, nucleation could occur either from liquid or from vapor. Because it is likely that $\gamma_{LV} > 2\gamma_{SL}$ in most cases, the fact that liquid condensates are rarely observed to freeze suggests that kinetic factors are controlling the process or that the contact angle exceeds 90°. Exceptions to this appear to be *neo*-pentanol and tetrabromomethane.[41,47] An alternative way of testing the predictions of eq 14 would be to study the behavior of liquid around the contact region when bulk liquid is cooled below the melting point, thus avoiding the possibility of evaporation.

In summary, this study of capillary condensation below the melting point suggests that the size of the liquid condensates is related to the equilibrium between vapor and supercooled liquid, modified by the reduction in chemical potential caused by the curved interface of the condensate. The model presented in previous work[23,24,41] is valid for the equilibrium between a liquid and a solid condensate, but it is likely that kinetic factors will often prevent the formation of solid condensates.

Acknowledgment. H.K.C. acknowledges V. V. Yaminsky for first suggesting to him that the liquid−vapor equilibrium should be the determinant of the condensate size. We thank A. M. Hyde from the Department of Applied Mathematics at the Australian National University for invaluable technical advice, M. Heuberger and J. Vanicek from the Department of Materials, ETH, Zurich for advice about the temperature-control system, staff of the Mechanical and Electronics Workshops in the School of Physics and Astronomy for technical assistance, and J. R. Henderson for helpful discussions. This research was supported by the EPSRC in the form of a DTA award for P.B. and Grant GR/R55450/01 for H.K.C.

References and Notes

(1) Christenson, H. K. *J. Phys.: Condens. Matter* **2001**, *13*, R95.
(2) Alba-Simionesco, C.; Coasne, B.; Dosseh, G.; Dudziak, G.; Gubbins, K. E.; Radhakrishnan, R.; Sliwinska-Bartkowiak, M *J. Phys.: Condens. Matter* **2006**, *18*, R15.
(3) Evans, R.; Marini Bettolo Marconi, U.; Tarazona, P. *J. Chem. Phys.* **1986**, *84*, 2376.
(4) Ball, P. C.; Evans, R. *Europhys. Lett.* **1987**, *4*, 715.
(5) Everett, D. H.; Haynes, J. M. *Z. Phys. Chem. (Frankfurt)* **1975**, *97*, 301.
(6) Gelb, L. D.; Gubbins, K. E. *Langmuir* **1998**, *14*, 2097.
(7) Israelachvili, J. N.; Adams, G. E. *J. Chem. Soc., Faraday Trans. 1* **1978**, *74*, 975.
(8) Parker, J. L.; Christenson, H. K.; Ninham, B. W. *Rev. Sci. Instrum.* **1989**, *60*, 3135.
(9) Tonck. A.; Georges, J. M.; Loubet, J.-L. *J. Colloid Interface Sci.* **1988**, *126*, 150.
(10) Kierlik. E; Monson, P. A.; Rosinberg, M. L.; Sarkisov, L.; Tarjus, G. *Phys. Rev. Lett.* **2001**, *87*, 055701.
(11) Fisher, L. R.; Israelachvili, J. N. *J. Colloid Interface Sci.* **1981**, *80*, 528.
(12) Israelachvili, J. N. *J. Colloid Interface Sci.* **1973**, *44*, 259.
(13) Barthel, E.; Lin, X. Y.; Loubet, J.-L. *J. Colloid Interface Sci.* **1996**, *177*, 401.
(14) Crassous, J.; Charlaix, E.; Loubet, J.-L. *Europhys. Lett.* **1994**, *28*, 37.
(15) Christenson, H. K. *Phys. Rev. Lett.* **1994**, *73*, 1821.
(16) Maeda, N.; Israelachvili, J. N. *J. Phys. Chem. B* **2002**, *106*, 3534.
(17) Maeda, N.; Israelachvili, J. N.; Kohonen, M. M. *Proc. Nat. Acad. Sci. U.S.A.* **2003**, *100*, 803.
(18) Kohonen, M. M.; Maeda, N.; Christenson, H. K. *Phys. Rev. Lett.* **1999**, *82*, 4667.
(19) Maeda, N.; Kohonen, M. M.; Christenson, H. K. *Phys. Rev. E* **2000**, *61*, 7239.
(20) Maeda, N.; Kohonen, M. M.; Christenson, H. K. *J. Phys. Chem. B* **2001**, *105*, 5906.
(21) Crassous, J.; Charlaix, E.; Loubet, J.-L. *Phys. Rev. Lett.* **1997**, *78*, 2425.
(22) Christenson, H. K. *J. Colloid Interface Sci.* **1985**, *104*, 234.
(23) Christenson, H. K. *Phys. Rev. Lett.* **1995**, *74*, 4675.
(24) Christenson, H. K. *Colloids Surf. A: Physicochem. Eng. Aspects* **1997**, *123*, 355.
(25) Maeda, N.; Christenson, H. K. *Colloids Surf., A* **1999**, *159*, 135.
(26) Xu, L.; Lio, A.; Hu, J.; Ogletree, D. F.; Salmeron, M. *J. Phys. Chem. B* **1998**, *102*, 540.
(27) Riedo, E.; Levy, F.; Brune, H. *Phys. Rev. Lett.* **2002**, *88*, 185505.
(28) Feiler, A. A.; Jenkins, P.; Rutland, M. W. *J. Adhes. Sci. Technol.* **2005**, *19*, 165.
(29) Sirghi, L.; Szoszkiewicz, R.; Riedo, E. *Langmuir* **2006**, *22*, 1093.
(30) Farshchi-Tabrizi, M.; Kappl, M.; Cheng, Y. J.; Gutmann, J.; Butt, H. J. *Langmuir* **2006**, *22*, 2171.
(31) Foote, H. W.; Saxton, B. J. *J. Amer. Chem. Soc.* **1916**, *38*, 588.
(32) Coolidge, A. S. J. *J. Am. Chem. Soc.* **1924**, *46*, 596.
(33) Patrick, W. A.; Land, W. E. *J. Phys. Chem.* **1934**, *38*, 1201.
(34) Batchelor, R. W.; Foster, A. G. *Trans. Faraday Soc.* **1944**, *40*, 300.
(35) See Petrov, O.; Furo, I. *Phys. Rev. E* **2006**, *73*, 011608, and references therein.
(36) Beamish, J. R.; Mulders, N.; Hikata, A.; Elbaum, C. *Phys. Rev. B* **1991**, *44*, 9314.
(37) Kondo, Y.; Schindler, M.; Pobell, F. *J. Low Temp. Phys.* **1995**, *101*, 195.
(38) Schindler. M.; Dertinger, A.; Kondo, Y.; Pobell, F. *Phys. Rev. B* **1996**, *53*, 11451.
(39) Earnshaw, J. C.; Hughes, C. J. *Phys. Rev. A* **1992**, *46*, 4494.
(40) Wu, X. Z.; Ocko, B. M.; Sirota, E. B.; Sinha, S. K.; Deutsch, M.; Cao, B. H.; Kim, M. W. *Science* **1993**, *261*, 1018.
(41) Qiao, Y.; Christenson, H. K. *Phys. Rev. Lett.* **2001**, *86*, 3807.
(42) Qiao, Y. Ph.D. Thesis, Australian National University, 2001.
(43) Asakawa, T.; Hisamatsu, H.; Miyagishi, S. *Langmuir* **1995**, *11*, 478.
(44) Heuberger, M.; Vanicek, J.; Zach, M. *Rev. Sci. Instrum.* **2001**, *72*, 3556.
(45) *Handbook of Chemistry and Physics*, 57th ed.; Weast, R. C., Ed.; CRC Press: Cleveland, OH, 1976.
(46) Chen, Y.-L.; Israelachvili, J. N. *J. Phys. Chem.* **1992**, *96*, 7752.
(47) Jackson, C. L.; McKenna, G. B. *J. Chem. Phys.* **1990**, *93*, 9002.
(48) Derjaguin, B. V. *Acta Physicochim. URSS* **1940**, *12*, 181.
(49) Evans, R.; Marini Bettolo Marconi, U. *Chem. Phys. Lett.* **1985**, *114*, 415.
(50) Qiao, Y.; Christenson, H. K. *Phys. Rev. Lett.* **1999**, *83*, 1371.
(51) Makkonen, L. *Langmuir* **2002**, *18*, 1445.
(52) Finke, H. L.; Scott, D. W.; Gross, M. E.; Messerly, J. F.; Waddington, G. *J. Am. Chem. Soc.* **1956**, *73*, 5469.
(53) Surface tension values of some common test liquids for surface energy analysis. http://www.surface-tension.de/ (accessed Jan 2007).